

The Mechanism of Heat Transfer in a Spray Column Heat Exchanger:

II. Dense Packing of Drops

RUTH LETAN and EPHRAIM KEHAT

Technion, Israel Institute of Technology, Haifa, Israel

Temperature profiles of water in a spray column heat exchanger, 15 cm. in diameter and 150 cm. long, operating with a dense packing of kerosene drops, were measured. The range of superficial velocities was 0 to 0.8 cm./sec. of water and 0.5 to 1.7 cm./sec. of kerosene. The bottom of the dense packing was either slightly above or 15 cm. below the bottom of the column proper.

The physical picture of heat transfer is similar to that for dispersed packings of drops and emphasizes the dominant role of wakes in the heat transfer mechanism. The mathematical equations for dispersed packings of drops were modified to take into account the reduction of wake size at the interface of the two packings and the difference in the mixing patterns at the top of the column. An empirical allowance for the effect of bypassing is suggested. The volume of the wakes and the rate of wake shedding were estimated from the temperature profiles. General agreement was found between the theory and the experimental data of this and three other studies.

The object of this work was to study the mechanism of heat transfer for a spray column operating with a dense packing of drops. A spray column can be operated at the same flow rates of the two phases with a number of modes of packings of drops. Which mode of packing of drops prevails depends on the rate of coalescence of drops at the upper interface, on the initial dispersion pattern of the continuous phase, on the method of building up of the packing in the column, and on the location of the upper interface (4). The more useful modes of packing were termed *dispersed packings* and *dense packings* of drops (8). For dispersed packings of drops, the average holdup of drops increases with increased flow rates of the two phases and is in the range of 0 to 55%. For dense packings of drops, the average holdup decreases with increased flow rates of the two phases and is in the range of 30 to 70% (8). The velocity of the drops is approximately uniform for dispersed packings but varies considerably for dense packings of drops in laboratory size columns (10).

A spray column can be used for direct contact heat transfer between two immiscible phases. Recent reviews of direct contact heat transfer are available (5, 12).

Letan and Kehat have recently (9) suggested a mechanism for heat transfer in a spray column for dispersed packings of drops, which was substantiated by measurements of the temperature profiles of the two phases in a spray column heat exchanger. The wakes of the drops play a dominant role in this mechanism. The drops are formed by breakup of liquid jets, and heat is transferred from the highly mixed drops to the forming wakes as the drops start to rise up the column. Along the major portion of the column length, elements of wakes are detached, mix with the continuous phase, and are replaced by liquid from the continuous phase, which exchanges heat with the drop on its way to the wake. In the region of the inlet of the continuous phase, a highly mixed zone exists, and streams coming out of this region are at the same temperature. In the coalescence zone, at the top of the column, the wakes are detached and flow back down to the mixing zone.

Owing to the presence of the mixing zone, a consider-

able temperature jump of the continuous phase takes place at the inlet of the continuous phase (6). This temperature jump can be minimized by the use of a very long column (9). It was noted earlier (3) that for comparable flow rates, the temperature jump was much smaller for a dense packing of drops than for a dispersed packing of drops. The use of a dense packing of drops would therefore result in a much shorter column for the same heat transfer specifications. On the other hand, the range of operating superficial velocities for a dense packing of drops is lower than for a dispersed packing of drops (5), and therefore a larger column diameter would be needed for a dense packing of drops for the same flow rates. Experience with both types of packings of drops has shown that in the same columns, and despite the requirement for lower flow rates, the amount of heat transferred is greater when a dense packing of drops is used, and, therefore, operation with a dense packing of drops is more desirable.

The mechanism of heat transfer for a spray column operating with a dense packing of drops is more complicated than for a dispersed packing of drops, owing to the existence of a considerable distribution of drop velocities and to bypassing drops and continuous phase near the wall of the column (10). It is possible to superimpose the equations for the velocity distribution over the equations for heat transfer. However the resultant equations are extremely complicated and are of little practical use, since for large diameter columns the radial distribution of velocities is negligible (10). Therefore, only simple, empirical corrections are suggested in the theoretical equations for the effect of the velocity distribution in laboratory sized columns. The theoretical equations for a dense packing of drops require an additional hydraulic parameter. The bottom of the dense packing extends above a small region of a dispersed packing of drops, and the wake size decreases sharply when the drops enter the dense packing. The wake size is, therefore, required as a parameter for each type of packing.

Another difficulty arose in the experimental part of the work. The traps, used to measure the drop temperatures

(7), caused considerable coalescence within the dense packing in the column and had to be removed. Therefore, temperature profiles of the water only could be measured. Despite these additional complications, the theoretical model gave consistent agreement with the experimental data of this and other studies.

THE PHYSICAL MODEL

A detailed visualization of the physical model and the general form of the temperature profiles for cooling drops is shown in Figure 1. A short length of dispersed packing is maintained at the bottom of the column proper, and the dense packing of drops extends to the upper interface.

The following features of this model are different from the physical model suggested for dispersed packings of drops (9):

1. Elimination of the intermediate zone, which disappeared also for dispersed packings at high holdups. Wake shedding starts at the beginning of the dense packing by the break up of the wakes at the packings interface.

2. A jump of the temperature of the continuous phase at the packings interface due to the break up of wakes and mixing of the shed parts with the continuous phase. Unlike the case of dispersed packings of drops, at $z = 0$, $t_{cs} \neq t_{co}$, and an additional parameter, the wake size for the dense packing of drops is required for the theoretical equations.

3. The mixing zone at the inlet of the continuous phase is small, due to the dispersion of the continuous phase by the drops at the high drop holdup. [This may also be partly due to the location of the inlet of the continuous phase in the present column, which is at the center top of the column and not over the sides and the top as in the earlier column (9).] In this small mixing zone the returning liquid from the wakes, detached in the coalescence zone, mixes with the incoming continuous phase, and there is relatively little heat transfer contribution from the drops and their wakes. The drops and their wakes equilibrate in temperature as the wakes are detached, and therefore the temperature of the dispersed phase, after coalescence, is slightly higher than at the top of the drop packing. The same phenomenon, but of negligible magnitude, was noted also for dispersed packings of drops.

Two new studies that give support to the wake model have appeared recently. Somer and Aykut (13) studied the heat transfer between single water drops falling through a hot Nujol bed. Their results indicated a completely mixed state for the drops. Magarvey and Maclatchy (11) studied the wake formation and wake shedding of single drops of organic liquids falling through water. They found that elements of wakes are shed and replaced periodically, that most of the mass transferred to the wake during its formation is carried in the wake, and that the rate at which mass is transferred from the drop to the ambient liquid in the wake growth zone is not very great.

THE MATHEMATICAL MODEL

The following assumptions are made: steady state, no heat losses, constant average physical properties of the liquids, constant average holdup for the dense packing of drops, constant average drop size, constant but different final wake size for dense and dispersed packing of drops, equal flow rates in and out of the wake, and plug flow of drops. The last assumption will be modified later.

For convenience, cooling drops rising in a spray column heat exchanger are described.

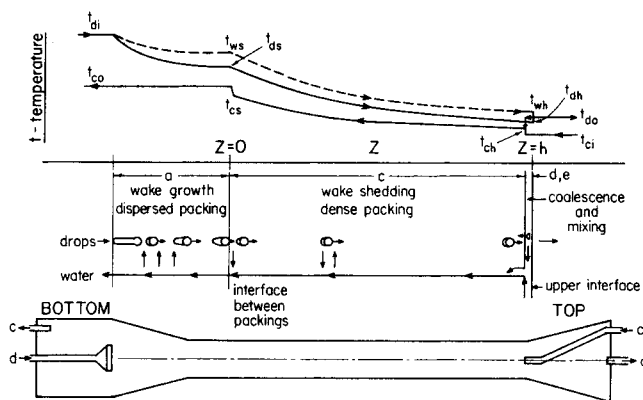


Fig. 1. Physical model of heat transfer in a spray column heat exchanger with a dense packing of drops.

Wake Growth Zone

The equations for the temperature of the continuous phase, drops, and wakes are identical with those for dispersed packing of drops (9), since wake growth takes place in the bottom region of dispersed packing.

At the interface of the two packings of the drops the drop temperature is [(9), Equation (4)]:

$$t_{ds} = (t_{di} - t_{co}) \exp\left(-\frac{M}{r}\right) + t_{co} \quad (1)$$

and the wake temperature is [(9), Equation (6)]:

$$t_{ws} = \frac{r}{M} (t_{di} - t_{co}) \left[1 - \exp\left(-\frac{M}{r}\right)\right] + t_{co} \quad (2)$$

As the drops cross the packings interface, part of the wakes is shed and mixes with the continuous phase.

Heat balance for the continuous phase at the packing interface (Figure 2a) gives

$$(V_c + M'V_d)t_{cs} + V_d(M - M')t_{ws} = (V_c + MV_d)t_{co} \quad (3)$$

where $V_d(M - M')$ is the continuous phase that was expelled from the wakes upon entering the dense packing. Eliminating t_{ws} from Equations (2) and (3) and using the definition

$$p = (1 + M'R)/R \quad (4)$$

we get

$$t_{cs} = t_{co} - \frac{r}{p} \left(1 - \frac{M'}{M}\right) \left[1 - \exp\left(-\frac{M}{r}\right)\right] (t_{di} - t_{co}) \quad (5)$$

Since the relative wake size for dispersed packings of drops (M) is known (9), and the continuous phase temperature at the packing interface (t_{cs}) can be measured, the relative wake size for the dense packing can be calculated from the continuous phase temperature profile by transforming Equations (4) and (5) into

$$M' = \frac{Rr \left[1 - \exp\left(-\frac{M}{r}\right)\right] - \frac{t_{co} - t_{cs}}{t_{di} - t_{co}}}{\frac{Rr}{M} \left[1 - \exp\left(-\frac{M}{r}\right)\right] + R \left(\frac{t_{co} - t_{cs}}{t_{di} - t_{co}}\right)} \quad (6)$$

Wake Shedding Zone

From a heat balance in the wake shedding zone, the change in the temperature of the continuous phase is

given by the same expression as for dispersed packings of drops (9), the only change being in the wake size. Therefore, from Equation (13) of (9)

$$\frac{dt_c}{dz} + \frac{m}{p} (t_w - t_c) = 0 \quad (7)$$

From this equation at $z = 0$ and $t_w = t_{ws}$, $t_c = t_{cs}$, the rate of wake shedding can be calculated from the slope of the temperature profile at $z = 0$:

$$m = \frac{p \left(-\frac{dt_c}{dz} \right)_s}{t_{ws} - t_{cs}} \quad (8)$$

where t_{ws} is calculated from the heat balance in the wake growth zone by Equation (2).

Similarly, all other derivations for the wake shedding zone for dispersed packings of drops can be used here [(9), Equations (8) and (11)]. The boundary condition at $z = 0$ is taken as $t_c = t_{cs}$ instead of $t_c = t_{co}$ for dispersed packings of drops, and the wake size is taken as M' . The three differential equations for t_c , t_d , and t_w can be solved simultaneously.

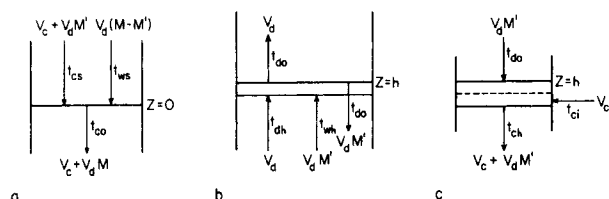


Fig. 2. Heat balances: a. Continuous phase at interface of packings. b. At coalescence interface. c. At the inlet of the continuous phase.

The final dimensionless temperature profiles in the wake shedding zone for drops, continuous phase, and wakes are

$$\theta_d = \frac{t_d - t_{co}}{t_{di} - t_{co}} = \left\{ \frac{m}{r} \left[\frac{1+S}{\alpha_1} (1 - \exp(\alpha_1 z)) - \frac{S}{\alpha_2} (1 - \exp(\alpha_2 z)) \right] + \frac{1}{1+N \left[\exp\left(\frac{M}{r}\right) - 1 \right]} \right\} \left[N + (1-N) \exp\left(-\frac{M}{r}\right) \right] \quad (9)$$

$$\theta_c = \frac{t_c - t_{co}}{t_{di} - t_{co}} = \left\{ \frac{m}{r} \left[\frac{1+S}{\alpha_1} \left(1 - \left[\frac{r}{m} \alpha_1 + 1 \right] \exp(\alpha_1 z) \right) - \frac{S}{\alpha_2} \left(1 - \left[\frac{r}{m} \alpha_2 + 1 \right] \exp(\alpha_2 z) \right) \right] + \frac{1}{1+N \left[\exp\left(\frac{M}{r}\right) - 1 \right]} \right\} \left[N + (1-N) \exp\left(-\frac{M}{r}\right) \right] \quad (10)$$

$$\theta_w = \frac{t_w - t_{co}}{t_{di} - t_{co}} = \left\{ \frac{m}{r} \left[\frac{1+S}{\alpha_1} \left(1 - \left[\frac{r}{m} \alpha_1 + 1 \right] \left[1 - \frac{p}{m} \alpha_1 \right] \exp(\alpha_1 z) \right) - \frac{S}{\alpha_2} \left(1 - \left[\frac{r}{m} \alpha_2 + 1 \right] \left[1 - \frac{p}{m} \alpha_2 \right] \exp(\alpha_2 z) \right) \right] + \frac{1}{1+N \left[\exp\left(\frac{M}{r}\right) - 1 \right]} \right\} \left[N + (1-N) \exp\left(-\frac{M}{r}\right) \right] \quad (11)$$

where

$$N = \frac{r}{p} \left(1 - \frac{M'}{M} \right) \quad (12)$$

$$\alpha_1 + \frac{m}{r} - \frac{m}{p} \left\{ \frac{\left(\frac{r}{M} + N \right) \left[\exp\left(\frac{M}{r}\right) - 1 \right]}{1+N \left[\exp\left(\frac{M}{r}\right) - 1 \right]} \right\} S = \frac{\alpha_2 - \alpha_1}{\alpha_2 - \alpha_1} \quad (13)$$

$$\alpha_1 = -\frac{m}{2} \left[\left(\frac{1}{M'} + \frac{1}{r} - \frac{1}{p} \right) + \sqrt{\left(\frac{1}{M'} + \frac{1}{r} + \frac{1}{p} \right)^2 - \frac{4}{M'r}} \right] \quad (14a)$$

$$\alpha_2 = -\frac{m}{2} \left[\left(\frac{1}{M'} + \frac{1}{r} - \frac{1}{p} \right) - \sqrt{\left(\frac{1}{M'} + \frac{1}{r} + \frac{1}{p} \right)^2 - \frac{4}{M'r}} \right] \quad (14b)$$

A simple check of these equations is to substitute $M = M'$. For this case, $N = 0$, and Equations (8) to (11), (13), and (14) become identical with the equivalent equations for a dispersed packings of drops (9).

Coalescence and Mixing Zone

A heat balance at the coalescence interface, assuming that all outgoing streams are at the same temperature (Figure 2b), gives

$$V_d (\rho C_p)_d t_{dh} + V_d M' (\rho C_p)_c t_{wh} = V_d (\rho C_p)_d t_{do} + V_d M' (\rho C_p)_c t_{do} \quad (15)$$

This equation and the definition of r , yield:

$$t_{do} = \frac{M' t_{wh} + r t_{dh}}{M' + r} \quad (16)$$

The detached wakes from the coalescence interface mix with the incoming continuous phase, slightly below the upper interface. Heat balance for this mixing process (Figure 2c) gives

$$V_c (\rho C_p)_c t_{ci} + V_d M' (\rho C_p)_c t_{do} = (V_d M' + V_c) (\rho C_p)_c t_{ch} \quad (17)$$

which can be rearranged to yield

$$t_{ci} = (1 + RM')t_{ch} - RM' t_{do} \quad (18)$$

The values of t_{dh} , t_{ch} , and t_{wh} can be calculated from Equations (9) to (11) at $z = h$. The value of t_{ci} can also be calculated from the three other end temperatures and a heat balance:

$$t_{ci} = t_{co} - Rr(t_{di} - t_{do}) \quad (19)$$

Since the mixing zone is very small, the length of the wake shedding zone is practically equal to the length of the dense packing.

From specified external temperatures at the bottom of the column and Equations (9) to (11), (16), and (18), the external temperatures at the top of the column can be calculated for the case of plug flow of drops. Conversely, the length of the dense packing h required, for specified external temperatures at the top and bottom of the column, can be calculated by iteration. For large diameter columns, where the assumption of no radial distribution of drop velocities holds, the above equations are exact. For small diameter columns, some modifications of the theoretical expressions are needed to allow for the deviation from plug flow of the drops.

OPERATION WITH A RADIAL DISTRIBUTION OF VELOCITIES OF DROPS

The pattern of flow of the drops for dense packings of drops is (10): a semiparabolic radial distribution of drop velocities in the core of the column and bypassing of drops and continuous phase near the wall. The velocity distribution in the core does not affect the wake size but probably affects the rate of wake shedding per unit time. Since the rate of wake shedding in the theoretical equations is defined per unit length, the velocity distribution in the core should not have a considerable effect on the validity of the theoretical equations, and this effect can be neglected relative to the effect of bypassing drops and continuous phase.

Each bypassing phase has negligible contact with the other phase, and an estimate of the outlet temperatures can be made, provided the degree of bypassing (x) is known.

The following assumptions are used:

1. The bypassing drops start at the packing interface

and do not shed elements of wakes or exchange heat before reaching the coalescence interface.

2. The bypassing continuous phase starts at the top temperature below the inlet (t_{ch}) and mixes with the rest of the continuous phase only below the dispersed packing of drops. Hence

$$t_{do} \text{ exp} = (1 - x_d) t_{do} \text{ calc} + x_d t_{ds} \text{ calc} \quad (20)$$

$$t_{co} \text{ exp} = (1 - x_c) t_{co} \text{ calc} + x_c t_{ch} \text{ calc} \quad (21)$$

The values of x_d and x_c can be calculated from these equations by iteration of $t_{co} \text{ calc}$, until $t_{ci} \text{ calc} = t_{ci} \text{ exp}$.

PARAMETRIC ANALYSIS OF THE THEORETICAL EQUATIONS

The theoretical equations developed in the previous sections can be used to calculate the relations between the operating end temperatures and the length of the wake shedding zone for five parameters: R , r , M , M' , and m . The effect of these parameters is discussed below.

It was shown for dispersed packings of drops (9) that the optimum ratio of thermal capacities of the two streams is unity. A similar analysis of the equations presented here yields the same results. It is, however, of interest to study this aspect quantitatively. Figure 3 shows the length of the wake shedding zone and the temperature approach at the top of the column, which were computed as function of r and R , for one set of operating temperatures and one set of wake parameters. Curves or lines for constant values of the ratio of thermal capacities of the two streams are also shown. The required length for the wake shedding zone increases sharply for values of $Rr < 1$, and the temperature approach at the top of the column increases sharply for values of $Rr > 1$. (The effect of the values of Rr on the temperature approach are the same for any countercurrent heat exchanger.) The optimum operating range of Rr is, therefore, at $Rr = 1$, and operation is still reasonable for slightly larger values of Rr .

A generalized plot of the effect of operating temperatures on the length of the wake shedding zone for $Rr = 1$ and one set of wake parameters are shown in Figure 4. The lines are actually curves, but the slopes increase by less than 0.2% along the curves. It is shown that a considerable penalty in column height is paid if a small tempera-

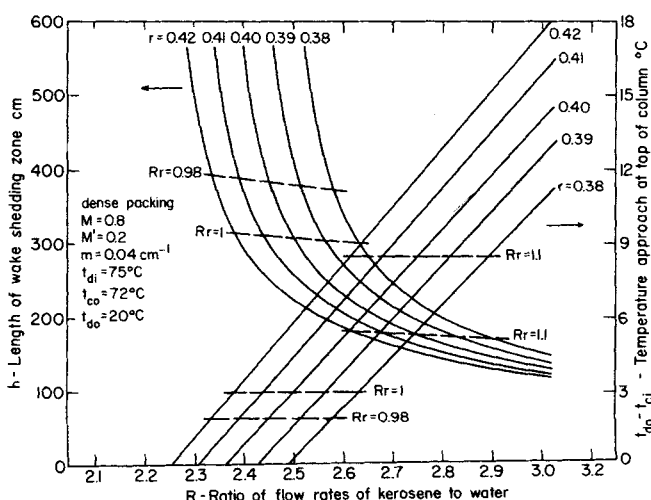


Fig. 3. The length of the wake shedding zone and the temperature approach at the top of the column as function of R and r .

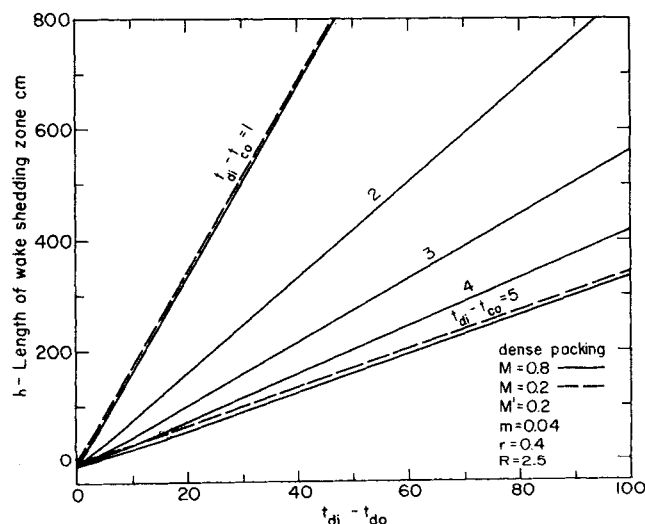


Fig. 4. The length of the wake shedding zone as function of the operating temperatures for $r = 0.40$ and $R = 2.5$.

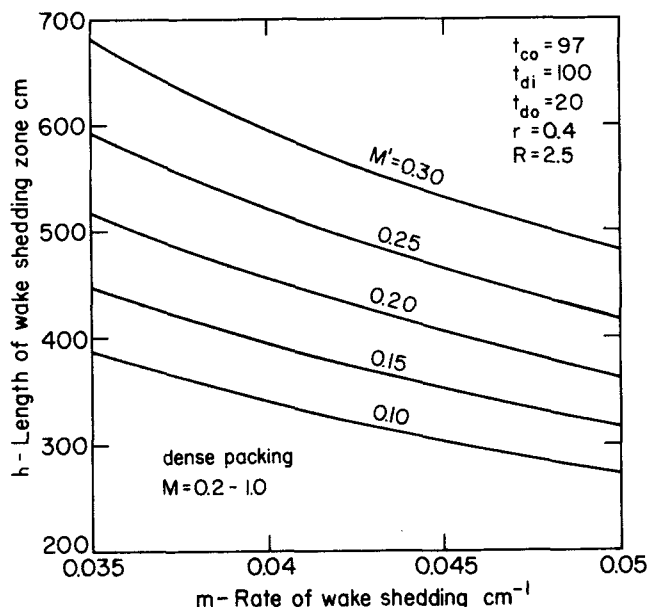


Fig. 5. The length of the wake shedding zone as function of the wake parameters for $r = 0.40$ and $R = 2.5$.

ture approach is desired. The slope of the lines in this plot is inversely proportional to the temperature approach. Therefore, the five lines of this plot can be generalized into a single line:

$$h = -13.49 + 17.87 \frac{t_{di} - t_{do}}{t_{di} - t_{co}} \quad (22)$$

For each set of the five parameters, one curve of h against $(t_{di} - t_{do}) / (t_{di} - t_{co})$ is obtained. For all combinations, when $Rr = 1$, these curves are practically straight lines.

The effect of the wake parameter M is extremely slight in the range of $M = 0.8$ to 1.2 and is negligible in the range of $M = 0.2$ to 0.8 as is shown by dashed lines in Figure 4. The effect of the other two wake parameters is shown in Figure 5. The length of the wake shedding zone decreases with decreased values of M and with increased values of m , since both effects lead to a larger number of exchanges of the wake volume up the column for the same column.

APPLICATION OF THE SUGGESTED MODEL TO THE CALCULATIONS OF VOLUMETRIC HEAT TRANSFER COEFFICIENT AND HTU

Commonly used representations of the rate of heat transfer in a spray column are the volumetric heat transfer coefficient (1, 2, 14) and HTU (2).

The volumetric heat transfer coefficient is defined as

$$U_v = \frac{V_c(\rho C_p)_c(t_{co} - t_{ci})}{L \Delta t_m} \quad (23)$$

where Δt_m , the nominal average driving force, is calculated by averaging the temperature approach at the ends of the columns.

The height of a transfer unit is defined as

$$\text{HTU} = \frac{L}{\int_L^0 \frac{dt_c}{\Delta t}} \quad (24)$$

where Δt is the local driving force.

A basic assumption inherent in the use of a mean driving force is that at any point along the spray column all the heat lost by one phase is gained by the other phase.

This assumption is not justified in this case in view of the temperature profiles and the physical model, since heat transferred from the drop to the wake is transferred to the continuous phase higher up the column. However, for one set of operating conditions of practical interest, the values of the volumetric heat transfer coefficient and HTU can be calculated from the theoretical equations as will be shown below, without utilizing the above assumption. These values can be used to check experimental data given in the form of volumetric heat transfer coefficients and to design spray column heat exchangers for the same limitations of operating conditions. These limitations are the use of a long spray column and a ratio of thermal capacities of unity ($Rr = 1$).

It was shown earlier that the optimum ratio of thermal capacities of the two phases is unity. For this case only, the driving force (the temperature approach) at both ends of the column is equal. If we define the average driving force as the average of the driving forces at the ends of the column

$$\Delta t_m = t_{di} - t_{co} = t_{do} - t_{ci} \quad (25)$$

then

$$-\theta_{ch} = \frac{t_{co} - t_{ch}}{t_{di} - t_{co}} = \frac{t_{co} - t_{ch}}{\Delta t_m} \quad (26)$$

For long columns, the temperature jump at the inlet of the continuous phase is negligible, and

$$t_{ch} = t_{ci} \quad (27)$$

Therefore

$$-\theta_{ch} = \frac{t_{co} - t_{ci}}{\Delta t_m} \quad (28)$$

From Equation (14) it can be shown that $\alpha_1 < 0$ and that for $Rr = 1$, $\alpha_2 = 0$. If the second exponential term in Equation (10) is expanded into a series, and $\alpha_2 = 0$, then

$$-\frac{S}{\alpha_2} \left(1 - \left[\frac{r}{m} \alpha_2 + 1 \right] \exp(\alpha_2 z) \right) = \frac{Sr}{m} + Sz \quad (29)$$

Since α_1 always has a negative value, and for very long columns ($z \rightarrow \infty$), we get

$$\exp(\alpha_1 z) \rightarrow 0 \quad (30)$$

For $z = h$ and Equation (29) and (30), Equation (10) is reduced to

$$\theta_{ch} = \frac{m}{r} \left\{ \frac{1+S}{\alpha_1} + \frac{Sr}{m} + Sh + \frac{1}{1+N \left[\exp\left(\frac{M}{r}\right) - 1 \right]} \right\} \left[N + (1-N) \exp\left(-\frac{M}{r}\right) \right] = a - Bh \quad (31)$$

where

$$a = \frac{m}{r} \left\{ \frac{1+S}{\alpha_1} + \frac{Sr}{m} + \frac{1}{1+N \left[\exp\left(\frac{M}{r}\right) - 1 \right]} \right\} \left[N + (1-N) \exp\left(-\frac{M}{r}\right) \right] \quad (32)$$

$$B = -\frac{mS}{r} \left[N + (1-N) \exp\left(-\frac{M}{r}\right) \right] \quad (33)$$

For the range of $M = 0.2$ to 1 , $M' = 0.1$ to 0.3 , and $m = 0.02$ to 0.06 , the range of values of a is -0.37 to -0.87 and of B is 0.0167 to 0.1143 .

Combining Equations (23), (28), and (31) and assuming that for long columns

$$h \cong L \quad (34)$$

we get

$$U_v = -V_c (\rho C p)_c \left(\frac{a}{h} - B \right) \quad (35)$$

Since for long columns $\frac{a}{h} \rightarrow 0$

$$U_v = B (\rho C p)_c V_c \quad (36)$$

B , which is defined by Equation (33), is a function of R , r , m , M , M' . Over a limited range (for constant B) and for $Rr = 1$, U_v should increase with increased flow rate of the continuous phase.

It will now be shown that B is the inverse of the height of a transfer unit. From a heat balance and Equation (23)

$$Q = U_v A L \Delta t_m = B (\rho C p)_c V_c A L \Delta t_m \\ = V_c A (\rho C p)_c (t_{co} - t_{ci}) \quad (37)$$

From Equations (24) and (37) and since $\Delta t = \Delta t_m$

$$\frac{1}{B} = L \frac{\Delta t_m}{t_{co} - t_{ci}} = \text{HTU} \quad (38)$$

Figure 6 is a plot of HTU as function of the wake parameters for $r = 0.4$ and $Rr = 1$. The effect of M is negligible. The effect of the other wake parameters is similar to that in Figure 5, since HTU is related to the height required for a complete exchange of the wake contents, though it is not equal numerically to M'/m . For $Rr = 1$, increased values of R decrease the values of HTU slightly similarly to the slight decrease of the wake shedding zone with increased values of R for $Rr = 1$ in Figure 3.

Numerical verification of the meaning of a long column as required to make true Equations (30), (27), and (35) was made.

For the range of $M = 0.2$ to 1.0 , $M' = 0.1$ to 0.4 , $m = 0.02$ to 0.06 , $r = 0.3$ to 0.6 , and $Rr = 1$, $\exp(\alpha_1 h) < 10^{-5}$ for values of $h > 200$ cm. Equation (30) is, therefore, easily satisfied.

Equation (27) cannot be satisfied as easily. For the same parameters, $h = 3,000$ cm. and a temperature approach of 5°C ., $t_{ch} - t_{ci} < 0.6^\circ\text{C}$. For $h = 3,000$ cm. and a temperature approach of 1°C ., $t_{ch} - t_{ci} < 0.12^\circ\text{C}$. Therefore, an extremely long column is needed to eliminate the temperature jump completely.

For about the same range of parameters, the values of a reported earlier in this paper are -0.37 to -0.87 . For $h = 1,000$ cm. $\left| \frac{a}{h} \right| < 10^{-3}$, which satisfies Equation (35).

EXPERIMENTAL

The experimental system was described in detail earlier (9). The experimental column was made of Pyrex, 15 cm. in diameter and 150 cm. long (10 cm. shorter than the earlier column) and insulated with rockwool. The major modifications were the change of the top section (4), which was in the shape of an inverted cone, and the location of the water inlet with radial dispersion holes at the bottom center of the top conical section. Kerosene was used as the dispersed phase and distilled water as the continuous phase. Both phases were mutually saturated and continuously recirculated. The kerosene dispersion nozzles were 1.5 mm. in internal diameter. The

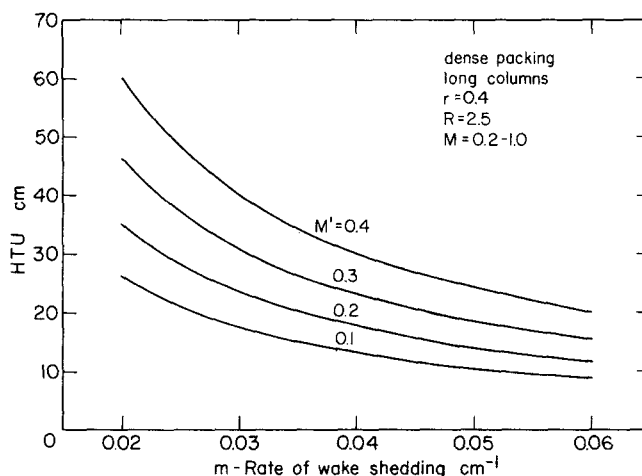


Fig. 6. HTU values as function of the wake parameters for $r = 0.40$, $R = 2.5$ and long columns.

drop size, physical properties, average holdup, and holdup distribution for this system were reported earlier (4, 8, 9).

The temperature profile of the water was measured by means of 11-30 gauge copper-constantan thermocouples, and the kerosene temperatures at the ends were measured by three similar thermocouples. The locations of the thermocouples are shown in Figure 8. Temperatures were recorded only after all thermocouples gave steady state readings. For each run the heat balance in both streams agreed to better than 10%. The accuracy of the readings of the thermocouples is estimated as 0.1°C . For most runs the average temperature in the column was 35°C ., and the inlet kerosene was about 15°C . warmer than the inlet water.

For an average temperature of 35°C ., $r = 0.39$. Since the great sensitivity of the results to variations of Rr was not known at the time, the experimental runs reported here were made for values of R of 2.18 to 2.75 to provide $Rr = 0.85$ to 1.07. Since a dense packing can be maintained only at the low flow rate range, the range of flow rates was 5 to 17 liters/min. of kerosene and 0 to 8 liters/min. of water (equivalent to $V_d = 0.5$ to 1.7 cm./sec. and $V_c = 0$ to 0.8 cm./sec.). The error in the measurement of flow rates was less than 5%. Sixteen runs were adequate to cover this range. These were made in two sets. In one set the bottom of the dense packing was kept (in most cases 10 cm.) above the bottom of the column proper, and in the other set the bottom of the dense packing extended 15 cm. into the bottom conical entry section. This was done in order to test an earlier conclusion, based on drop and holdup distribution data (4), that the lower conical entry section can be eliminated for dense packings of drops.

THERMAL PERFORMANCE OF THE COLUMN

The experimental results are plotted in Figure 7 as the ratio of the temperature change of the water to the average driving force at the ends of the column, as function of the total flow rate of the two phases per unit area. Since the same column was used in all these runs ($L = \text{const}$), the plotted parameter is equivalent to the parameter B , as can be seen by rearranging Equation (38) to yield

$$\frac{t_{co} - t_{ci}}{\Delta t_m} = BL \quad (39)$$

Since the number of transfer units is $L/\text{HTU} = LB$, it can be seen that if a very long column, plug flow, and $Rr = 1$ were used, this parameter would also equal the number of transfer units.

For the runs, where the bottom of the dense packing was within the column proper, a maximum thermal performance was obtained at total flow rates of 1.55 to 1.95 cm./sec. (and holdups of 0.5 to 0.6). At these flow rates,

TABLE 1. COMPARISON OF THE EXPERIMENTAL DATA WITH THE THEORY

Run	h , cm.	R	Experimental		Experimental		Calculated		$100 \times$ $\frac{t_{ci} \text{ calc} - t_{ci} \text{ exp}}{(t_{co} - t_{ci}) \text{ exp}}$	x_d	x_c
			t_{di} , °C.	t_{co} , °C.	t_{do} , °C.	t_{ci} , °C.	t_{do} , °C.	t_{ci} , °C.			
1	140	2.40	46.5	44.3	33.7	30.1	31.34	30.11	0.07	—	—
2	140	2.35	43.7	41.5	30.4	28.8	29.61	28.59	-1.7	—	—
3	145	2.38	42.6	39.5	31.3	28.7	21.38	19.81	-83.2	0.116	0.103
4	150	2.7	42.1	39.0	33.3	28.7	5.13	0.07	-227.9	0.184	0.178
5	140	2.45	46.4	42.8	32.5	28.9	19.66	17.25	-51.13	0.068	0.061
6	140	2.18	44.9	42.1	31.1	28.9	30.77	30.08	8.97	—	—
$M = 0.8$			$M' = 0.2$	$m = 0.04 \text{ cm.}^{-1}$		$r = 0.39$					

bypassing is minimal. The increase of the thermal performance with increased flow rates, at low flow rates is due to the decreased bypassing with increased flow rates (10). The decrease of thermal performance at higher flow rates is due to the decreasing holdup at higher flow rates (8). At the highest flow rates, the dense packing is indistinguishable from dispersed packing (8), with its poorer thermal performance. At these flow rates a dense layer of drops is formed in the conical bottom section, and there-

fore the two curves in Figure 3 tend to coincide at high flow rates. The existence of a maximum value of the volumetric heat transfer coefficient as function of the flow rates was also noted earlier (3).

For the runs, where the bottom of the dense packing was within the bottom conical section, the thermal performance was considerably poorer. This reiterates the earlier conclusion (4) that the conical bottom section can be dispensed with and replaced with a straight extension of the column proper, as was done successfully by Woodward (14) and by Greskovitch et al. (2).

THE TEMPERATURE PROFILES

A typical temperature profile is shown in Figure 8. This is one of the runs with the best thermal performance in Figure 7. The two parameters M' and m , used in Figure 3 were calculated from three of the runs with the best thermal performance by Equations (6) and (8) with the inherent assumption of no bypassing for these runs. The values of M for dispersed packing of drops are known (9). The accuracy of the measurement of the slope of the temperature profile is poor, and the estimated error in the values of m is 25%. Direct measurement of the rate of wake shedding by tracer technique will be made in the future.

The values of the wake parameters were

$$M = 0.8, \quad M' = 0.2, \quad \text{and} \quad m = 0.04 \text{ cm.}^{-1}$$

The values of these parameters for the other runs are highly influenced by bypassing of the two phases and therefore have no general significance. This limits the application of the theoretical equations to experimental runs with the highest thermal performance. However, once agreement of the theoretical equations with these experiments is shown, the theoretical equations can be used for the design of large diameter columns, for which bypassing is negligible (10), for the whole operational range.

The above values of the wake parameters were used to calculate the top temperature from the bottom temperatures for some of the runs in the upper curve in Figure 7. The results are presented in Table 1. The values of x_c and x_d were also calculated for the runs where bypassing was predominant. They range between 0.061 and 0.184, showing the considerable bypassing that took place for these runs. The agreement of the three runs with minimal bypassing (runs 1, 2, and 6) with the theoretical equations is good.

COMPARISON WITH DISPERSED PACKING OF DROPS

It was stated in the introductory section that despite the lower flow rates, more heat is transferred for a dense

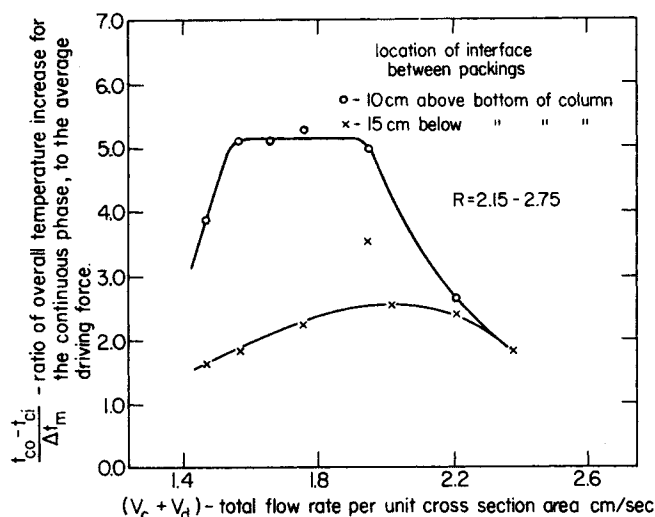


Fig. 7. Thermal performance of the column as function of the total flow rate of both phases and the location of the bottom of the dense packing.

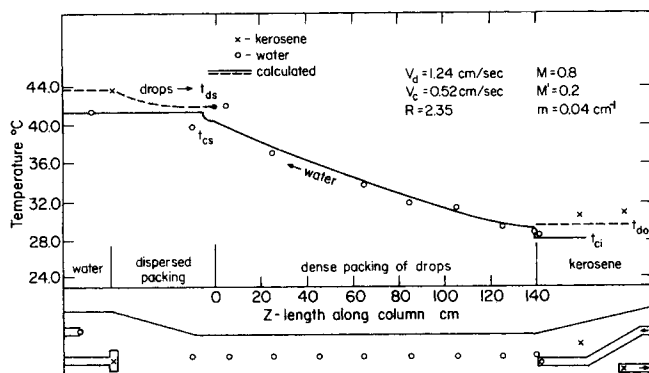


Fig. 8. Experimental and calculated temperature profiles of water for a dense packing of cooling drops and an average temperature of 35°C. (run number 2).

packing of drops than for a dispersed packing of drops in the same column. This statement can be substantiated by the results of this work.

As an example, the data of run 2 will be used. For the conditions of this run, $R = 2.35$, $t_{co} = 41.5^\circ\text{C}$., $t_{di} = 43.7^\circ\text{C}$., $h = 140$ cm.

For a dense packing of drops, $t_{ci} = 28.8^\circ\text{C}$. For a dispersed packing of drops, $t_{ci} = 37.36^\circ\text{C}$. [calculated according to (9)]. The ratio of heat throughputs for this case for the same throughput is

$$\frac{(t_{co} - t_{ci}) \text{ dense}}{(t_{co} - t_{ci}) \text{ dispersed}} = \frac{(41.5 - 28.8)}{(41.5 - 37.36)} = 3.04$$

According to Figure 6 of (8), the maximum velocity of the continuous phase for the same value of R is $V_c = 0.80$ cm./sec. for a dispersed packing of drops. According to Figure 8 of (4), the maximum velocity of the continuous phase for the same value of R is $V_c = 0.58$ cm./sec. for a dense packing of drops. Hence, for the maximum throughputs possible with each type of packing

$$\frac{[V_c(t_{co} - t_{ci})] \text{ dense}}{[V_c(t_{co} - t_{ci})] \text{ dispersed}} = \frac{0.58}{0.80} \times 3.04 = 2.2$$

A dense packing of drops will carry more than twice the heat throughput of a dispersed packing of drops for the conditions of this run.

APPLICATION TO OTHER STUDIES

Only three other studies in the literature report data on heat transfer in a spray column operated with a dense packing of drops.

Woodward (14) used a 4 in. column, 176 cm. long, shell fluid A, dispersion holes 1.6 mm. in diameter, and a thermal capacities ratio close to unity. His data are reported in the form of temperature differences. All his runs were in the best velocity range of $V_c + V_d = 1.6$ to 1.9, so that flow of the drops with minimal bypassing was probably taking place.

Since $Rr \approx 1$, it was assumed that his reported Δtm is equal to $t_{di} - t_{co}$. The length of the wake shedding zone was assumed to be 150 cm. The wake parameters of this work were assumed to hold with one exception. Since his drops were larger, they can accommodate a larger relative wake size in the dense packing region; therefore $M' = 0.30$ was assumed. Equations (9), (11), and (16) were

combined to give

$$t_{di} - t_{do} = \Delta tm \left(1 - \frac{M'\theta_{wh} + r\theta_{dh}}{M' + r} \right) \quad (40)$$

Equations (9), (11), and (40) were used to calculate $t_{di} - t_{do}$ for comparison with his data. The results are shown in Table 2. The agreement of the experimental data and the calculated data is good. The outstanding poor agreement is for run 1, where from the low holdup it appears possible that the column was operated with a dispersed packing of drops, with its poorer efficiency for this run.

Bauerle and Ahlert (1) used a 9 in. column, 10 ft. long, octane, a dense packing of drops, a variable length of the dense packing, one flow rate — $V_c = 57$ ft./hr., $R = 3.2$, and $r = 0.31$ ($Rr \approx 1$). Their data are presented in the form of volumetric heat transfer coefficients. For the wake parameters of this work and the conditions of their work, $B = 1.92$ ft.⁻¹. From Equation (36), $U_v = 6,750$ B.t.u./ (hr.) (sq.ft.) (°F.). For their injector size of 1/16 in., which is the closest to the size used in this work, the maximum values of the volumetric heat transfer coefficient were $U_v = 6,000$ to 6,500 which are in good agreement with the calculated value.

Bauerle and Ahlert (1) also found a linear relationship between the volumetric heat transfer coefficient and the average holdup as they varied the length of the dense packing. This relationship can also be developed from the theoretical equations. If the holdup of the dispersed packing below the dense packing of drops can be neglected, relative to the much higher holdup of the dense packing, for the range of velocities of the two phases in that study

$$H_{\text{avg}} = H_{\text{dense}} \frac{h}{L} \quad (41)$$

where h/L is the fraction of the column, with a dense packing of drops. For $Rr = 1$, and repeating the derivation of Equation (35) for $h \neq L$, we get

$$U_v = -V_c (\rho C p)_c \left(\frac{a}{h} - B \right) \frac{h}{L} \equiv V_c (\rho C p)_c B \frac{h}{L} \quad (42)$$

Combining with Equation (41) we get

$$U = \frac{V_c (\rho C p)_c B}{H_{\text{dense}}} H_{\text{avg}} \quad (43)$$

Since all other factors were constant in their work, the

TABLE 2. ANALYSIS OF WOODWARD'S (14) DATA

Run	H	R	Δtm	$t_{di} - t_{do}, \text{exp}$	$t_{di} - t_{do}$	$100 \times$
					calc	$\frac{(t_{di} - t_{do})_{\text{calc}} - (t_{di} - t_{do})_{\text{exp}}}{(t_{di} - t_{do})_{\text{exp}}}$
1	0.20	2.46	4.07	16.20	27.90	72.5
2	0.35	2.53	2.80	17.30	20.99	21.3
3	0.40	2.53	2.45	17.60	18.36	4.3
4	0.44	2.56	2.35	17.70	18.29	3.4
5	0.50	2.54	2.20	18.00	16.70	-7.2
6	0.54	2.52	2.15	18.33	15.91	-13.2
7	0.57	2.63	2.18	17.80	18.54	4.2
8	0.56	2.70	2.20	17.30	18.31	-8.5
9	0.56	2.53	2.53	17.43	18.96	8.8
10	0.56	2.43	2.67	17.70	17.66	-0.2

Distribution holes — 1.6 mm., Column length — 176 cm., Shell A-Water, $r = 0.4$
Assumed: $h = 150$ cm., $M = 0.8$, $M' = 0.3$, $m = 0.04$ cm.⁻¹

volumetric heat transfer coefficient should vary linearly with the average holdup.

Greskovich et al. (2) report thirteen runs with a dense packing of drops. They used kerosene and water, three columns 7 ft. and 10 ft. 6 in. in diameter and 10 ft. 4 in. in diameter, and $Rr \cong 1$. Most of their runs were for a high range of $V_c + V_d = 2.0 - 4.1$ cm./sec. which, according to Figure 7, is a poor operating range with a considerable distribution of velocity of drops. Moreover, in this range the holdup decreases up the column (4). It is not surprising, therefore, that volumetric heat transfer coefficients calculated from their data are about one-half of those calculated from the theoretical equations, similar to the runs of this study in the same velocity range.

Qualitatively, the effects of the parameters of their work are in line with what the theory predicts. The volumetric heat transfer coefficients increase with increased V_c for all their runs. The decrease in column diameter increases the variance of residence times of the drops (10) with resultant poorer thermal performance of the narrower column.

Since the lengths of the region of dispersed packing and the mixing and coalescence zones are independent of the column length, the relative increase in the length of the wake shedding zone, when the length of the column is increased from 7 to 10 ft., is larger than the relative sizes of the columns, and therefore the values of HTU increase slightly for the longer column. All these effects are consistent with the predictions of the proposed physical model.

CONCLUSIONS

The proposed physical model may be criticized as using essentially two parameters: M' and m instead of the conventional volumetric heat transfer coefficients or HTU. However, it is consistent with the known effects of the wakes of drops, and despite the complications introduced by the velocity distribution of the drops in laboratory sized columns, the physical model shows good agreement with the experimental results of this and other works, whereas the volumetric heat transfer coefficients reported in the literature cannot be correlated to cover all the published studies.

The real test of this model will come when quantitative values of the wake parameters are available. It is planned to conduct such studies in the near future.

The most important conclusion of this study is that heat transfer in a spray column operating with a dense packing of drops, similar to operation with a dispersed packing of drops, is controlled by the fluid mechanics of the system and not by the resistance to heat transfer inside or at the surface of the drops.

The thermal performance of small diameter columns is reduced significantly by the effect of bypassing and is also reduced if the bottom of the dense packing of drops is maintained within the conical bottom entry section.

Volumetric heat transfer coefficients may be used for correlation or for design of column heights only for long columns and for a ratio of thermal capacities of the two phases of unity.

ACKNOWLEDGMENT

This work was supported by the Israel National Council for Research and Development.

NOTATION

- A = internal area of column, sq.cm.
 a = defined by Equation (32)
 B = defined by Equation (33), cm.⁻¹

- C_p = heat capacity, cal./(g.) (°C.)
 H = holdup
 h = length of dense packing or of wake shedding zone, cm.
 HTU = height of a transfer unit, cm.
 L = length of column, cm.
 M = ratio of wake to drop volume for dispersed packings of drops
 M' = ratio of wake to drop volume for dense packings of drops
 m = volume of wake elements shed per volume of drop and unit length of column cm.⁻¹
 N = defined by Equation (12)
 p = $(1 + M'R)/R$
 Q = rate of heat transfer, cal./sec.
 R = V_d/V_c
 r = $(\rho C_p)_d/(\rho C_p)_c$
 S = defined by Equation (13)
 t = temperature, °C.
 Δt = local temperature driving force, °C.
 Δtm = nominal average temperature driving force, °C.
 U_v = volumetric heat transfer coefficient, B.t.u./(hr.) (cu.ft.) (°F.)
 V = flow rate per unit cross-section area, cm./sec.
 x = fractional bypassing
 z = distance along dense packing, cm.
 α = defined by Equation (14), cm.⁻¹
 θ = dimensionless temperature
 ρ = density, g./cc.

Subscripts

- avg = average
 c = continuous phase
 $calc$ = calculated
 d = dispersed phase
 exp = experimental
 h = at coalescence interface
 i = at inlet
 o = at outlet
 s = at bottom of dense packing
 w = wake

LITERATURE CITED

1. Bauerle, G. L., and R. C. Ahlert, *Ind. Eng. Chem. Proc. Design Develop.*, **4**, 225 (1965).
2. Greskovich, E. J., Paul Barton, and R. E. Hersh, *AIChE J.*, **13**, 1160 (1967).
3. Kehat, Ephraim, and Ruth Letan, report presented to the Israel National Council for Research and Development (Dec., 1963).
4. ———, *Ind. Eng. Chem. Proc. Design Develop.*, **7**, 387 (1968).
5. Kehat, Ephraim, and Samuel Sideman, "Direct Contact Liquid-Liquid Heat Transfer," accepted for publication in *Recent Advances in Liquid-Liquid Extraction*, C. Hanson, ed., Pergamon Press, London, England (1970).
6. Letan, Ruth, and Ephraim Kehat, *AIChE J.*, **11**, 804 (1965).
7. ———, *Chem. Eng. Sci.*, **20**, 856 (1965).
8. ———, *AIChE J.*, **13**, 443 (1967).
9. *Ibid.*, **14**, 398 (1968).
10. *Ibid.*, **15**, 7 (1969).
11. Magarvey, R. H., and C. S. Maclatchy, *ibid.*, **14**, 260 (1968).
12. Sideman, Samuel, "Advances in Chemical Engineering," Vol. 6, p. 207, Academic Press, New York (1966).
13. Somer, T. G., and Muruvvet Aykut, *Brit. Chem. Eng.*, **12**, 1088 (1967).
14. Woodward, Teynham, *Chem. Eng. Progr.*, **57**, No. 1, 52 (1961).

Manuscript received November 4, 1968; revision received March 12, 1969; paper accepted March 17, 1969.